

Sandeep Kuriakose^{1*}, Salvatore Cataldo¹, Paolo Parenti¹, Massimiliano Annoni¹

¹Politecnico di Milano, Department of Mechanical Engineering, 20156, Milan, Italy

Abstract

Recent developments showed that micro extrusion of feedstock can be used for manufacturing metallic micro bi-lumen tubes of very high length-to-diameter aspect ratios which are not viable by conventional metal extrusion or commonly used feedstock processing technologies like injection moulding or hot pressing. The extrusion of high aspect ratio micro components faces the challenge of maintaining the geometrical accuracy, surface finish and structural properties as the micro extrusion in green-state is followed by debinding and sintering operations which result in shrinkage and variations in surface finish and structure. The stages of the process chain such as solvent/thermal debinding, to remove the polymeric binder, and pre-sintering, to achieve a mild structural rigidity before the part sintering, are critical stages in achieving the surface and structural properties in case of high aspect ratio micro parts and are not yet studied in case of micro extrusion of feedstock. In this study, the effect of debinding and pre-sintering on surface and structural properties of bi-lumen tubes processed at different extrusion conditions are discussed. Surface roughness of the tubes is analysed using 3D microscopy and structural properties are studied using scanning electron microscopy (SEM) and electric discharge spectroscopy (EDS). The debinding and pre-sintering experiments on extruded micro bi-lumen tubes retained very good surfaces without any cracks or defects. The study showed that interactions of extrusion temperature and extrusion velocity influence the surface finish of the extruded tubes the most. The sintered bi-lumen samples showed a good areal surface finish, Sa of 2.21 μm which is near to the green-state value confirming the suitability of the applied debinding and pre-sintering parameters.

Keywords: micro extrusion, debinding, pre-sintering, bi-lumen tube, surface quality, feedstock.

1. Introduction

Micro extrusion is a processing methodology uniquely used for manufacturing very high length-to-thickness aspect ratio components specially for various bio-medical and micro fluidic applications. The recent studies by the authors showed that extrusion of feedstock is a revolutionary technique to manufacture micro metallic bi-lumens tubes of very high aspect ratio (length/diameter > 100), which are unachievable by conventional metal extrusion processes and other processing methodologies [1]. Metallic feedstock is a mixture of metal and polymeric binder. It is extruded [2] to the shape of bi-lumen tubes of required diameters and lengths. These tubes in green-state (Green) are then debinded and sintered to remove the polymeric binder and to get the required strength respectively [3].

The debinding, which is generally executed as solvent/water debinding (WD) or thermal debinding (TD) or both together one after other, is an important step for the dimensional accuracy, structural properties and strength in case of both metallic and ceramic micro components produced by feedstock processing [1,3]. The binder removal percentage also decides for the geometrical shape of the extruded bi-lumen tubes as it results in part shrinkage. The study of debinding processes in injection moulded parts showed that lower binder removal percentages during WD and TD result in cracking of the surface and thereby high surface roughness during the sintering stage [4]. The near complete removal of binder is important also to minimize the carbon content of the final sintered part and decides for its density, structural properties [5] and corrosion resistance, especially for the components used in the medical field [6].

The solvent debinding parameters, such as solvent temperature and debinding time, and thermal debinding parameters, such as debinding temperature, heating rates and holding time, influence the

component's surface finish and structural properties significantly [4,7]. The pre-sintering (PS) process, which is usually carried out after TD, is a necessary step to ease the transport of the very fragile parts after TD. In fact, they have to be put in a clean furnace to minimize the carbon pollution especially in case of micro components that need high density with low corrosion after the sintering process [6,8]. Due to the above reasons, understanding the variations of component properties and finding optimum levels of parameters for WD, TD and PS processes is very essential for high aspect ratio micro extruded parts [4-7]. Moreover, there is a lack of knowledge in this field as feedstock extrusion is relatively a new member of the feedstock processing methodologies. In this study, surface roughness (Sa) and structural property variations of extruded micro bi-lumen tubes processed with different extrusion processing conditions (i.e. extrusion temperature (Te) and extrusion velocity/screw speed (Ns)) are studied during WD, TD and PS to detect relationships among these processes.

2. Materials and methods

2.1 Material

The feedstock material chosen for the experimental investigation is a commercial feedstock, 17-4PH G120E from Polymim GmbH, Germany. The SEM and EDS analysis of the feedstock demonstrated its homogeneity in terms of distribution of the constituting elements of this biocompatible steel (15-17.5% Cr, 3-5% Ni & Cu, 1% Mn & Si and 0.07% C). The SEM analysis (Fig. 1) generally showed steel particles of globular shapes with most of the particle diameters below 10 μm and with particle size varying from 1 to 30 μm . The binder content of the feedstock must be treated with WD (solvent temperature $\leq 60^\circ\text{C}$) followed by TD (debinding temperature $\approx 600^\circ\text{C}$) to be removed.

2.2 Experimentation

The workpiece samples used for debinding and pre-sintering studies are manufactured by extrusion of feedstock by varying the extrusion parameters, extrusion temperature and extrusion velocity as shown in Table 1. The previous studies of authors showed that extrusion temperature and extrusion velocity are the key extrusion parameters in case of feedstock extrusion which determine the properties of the extruded bi-lumen tubes.

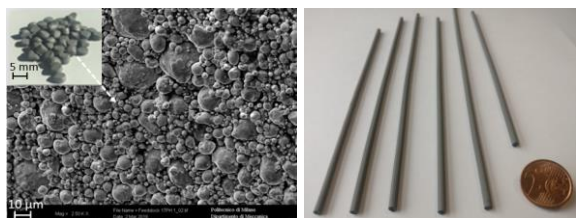


Fig. 1. 17-4PH G120E feedstock pellets and SEM image (left) and micro bi-lumen tubes (length = 125 mm) extruded in Green at 6 different extrusion conditions (right)

Table 1. Extrusion process parameters

Parameter	Levels	Replications
Temperature (Te) (°C)	140,150,160	4
Speed (Ns) (rpm)	22, 24	

A total of 24 samples of 3.18 mm nominal tube diameter, 0.7 mm lumen diameter and 125 mm length were extruded for all the 6 experimental combinations for 4 replicates. The extruded bi-lumen tubes in Green are shown in Fig. 1. A single screw extruder (Gimac s.r.l., Italy) with a 12 mm screw diameter is used with a die and pin of the mentioned nominal diameters of the bi-lumen tube is used for the feedstock micro extrusion. For studying the variation of surface and structural properties and at the same time to minimize the breakage of the tubes in each stage of the process chain, the following methodology is used (see Fig. 2). One sample (original length of 125 mm) from each of the 4 replicates of the 6 extrusion experimental combinations is selected and cut in two parts (100 mm + 25 mm). All the samples (of length 125 mm, 100 mm, 25 mm) are water debinded in a tank with distilled water. The 25 mm samples (one for each of the 6 extrusion combinations) were collected after WD for % Removal, Sa and SEM analysis. Remaining tubes are thermal debinded and pre-sintered. The samples of 100 mm were collected for the analysis after TD/PS considering the extremely fragile nature of the bi-lumen tubes at the PS state. The remaining samples of 125 mm were kept for future sintering studies.

2.3.1 Water debinding

All the samples are water debinded in a debinding setup using distilled water and 2 % INHIBITOR 4000 (Zschimmer & Schwarz GmbH, Germany) corrosion inhibitor. The debinding equipment has a heater and a motor to maintain the temperature and circulation of the water uniform. A higher value of solvent temperature increases the binder removal rate but may result in cracking of the micro parts due to the increased transfer rate of polymeric binder. A lower value of solvent temperature improves the surface properties, but reduces the binder removal, increases

the debinding time and the processing cost. The WD parameter values, solvent temperature of 50 °C and debinding time of 72 hrs were selected considering the micro lumens of the bi-lumen tube [4]. Water debinding was done in two stages, first for debinding time of 48 hrs and then for another 24 hrs. Samples after debinding in each stage are dried in vacuum for 2 hrs at 70 °C and 1 hr at 100 °C, later cooled down to 70 °C switching off the furnace and then to room temperature by opening the furnace door to atmospheric temperature. The weight of the small pieces (25 mm) are measured after drying to calculate the percentage weight removal (% Removal) of the binder.

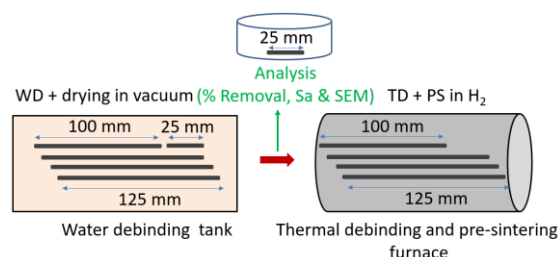


Fig. 2. The methodology used for WD and TD/PS.

2.3.2 Thermal debinding/Pre-sintering and Sintering

The TD and PS operations are done one after the other. TD is done by heating the samples to thermal debinding temperature of 600 °C, at heating rates of 3°C/min and holding time of 2.5 hrs. A small heating rate was selected for the TD process to prevent surface defects as the binder back bone polymer vapours escape from the tubes by heating [4], considering the micro lumens and high aspect ratio of the bi-lumen tubes. The TD and sintering were decided to be done in separate furnaces to minimize the possible contamination of samples to comply with the biomedical use for which the tubes may find applications in the future [5,6]. The PS operation follows TD in the same TD furnace, at a higher heating rate of 4°C/min to PS temperature of 800 °C and maintained there for a PS holding time of 1 hr followed by natural slow cooling by switching off the furnace heaters. A PS temperature of 800 °C and holding time of 1 hr are selected to avoid a partial sintering as the 17-4PH starts sintering above 900 °C and sintering effect increases with higher holding time. A Graphite tubular furnace (Proba s.r.l., Italy) with H₂ atmosphere is used for the TD/PS cycle. The H₂ atmosphere is selected for the PS activity as H₂ or Vacuum were found to be less corrosive for the sintered parts. Bi-lumen tubes are placed on Alumina plates as Alumina is inert and maintains its structural rigidity in the operated temperature range. The 100 mm long selected tubes were further sintered in a Vacuum furnace, TAV TS 150/250 (TAV S.p.a., Italy) at a higher heating rate of 5 °C/min to a sintering temperature of 1380 °C and for a sintering holding time of 2 hrs to evaluate the final properties.

The bi-lumen samples at Green, WD, TD/PS states were analysed to assess deviations of their surface roughness and structural properties. The % Removal of binder with respect to WD and TD/PS are analysed by measuring weight at each stage. The Sa of the tubes are evaluated by acquiring a surface of 1000 x 1000 μm² at 2 points along the length direction and 2 points around the circumferential direction of the tube. This strategy was adopted to understand the roughness variations along the length and

circumferential directions. A focus variation optical 3D microscope (Alicona GmbH, Austria) with 20X lens, a vertical resolution of 0.08 μm and a horizontal resolution of 2.5 μm was used for the acquisition. The acquired data clouds of the surface are form-removed using a cylindrical function and S_a was calculated by using a filter of 150 μm (15 % of 1000 μm). The structural property variations of bi-lumen tubes such as particle bonding, carbon content, porosity etc. are analysed using SEM (Zeiss, Germany) with an attached EDS (Oxford instruments, UK).

3. Results and discussion

The tubes after WD and PS maintained their shape without any deformation. The % Removal of binder with respect to WD and TD/PS and the variation of bi-lumen tube's surface roughness and structural properties with respect to the variation of extrusion parameters at Green, WD and PS are analysed.

3.1 Effect of WD and PS parameters on % Removal of binder.

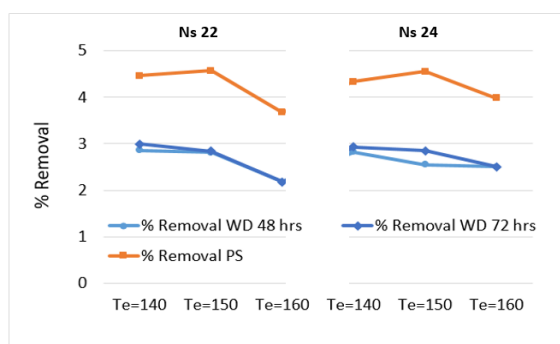


Fig. 3. % Removal of binder with respect to WD and PS

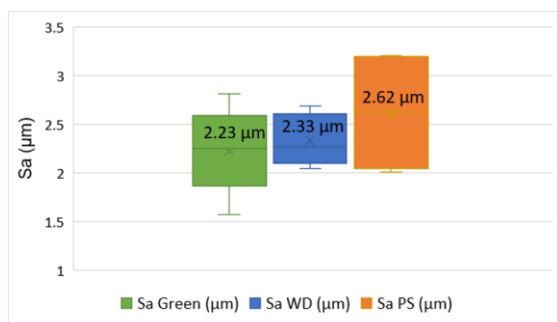


Fig. 4. S_a variation with respect to WD and PS

The analysis of the weight measurements of WD samples during the WD study showed a % Removal of binder with respect to debinding time as shown in Fig. 3. An average % Removal of 2.61 % was observed for 48 hrs of WD at 50 °C. The average % Removal value at 72 hrs was 2.71 %, with a very negligible 0.10 % average removal in the second 24 hrs of WD stage as seen in the Fig. 3. There was no observable difference for the bi-lumen tube surfaces in each of these stages. This fact displayed that water debinding time of 48 hrs itself removes the major part of the water soluble binder component. A small % Removal in the following 24 hrs showed that debinding time of 48 hrs or less could be enough for the WD. The graph of Fig. 3 shows that % Removal in case of tube processed at

high extrusion temperature of 160 °C (for constant Ns) was slightly lower. This effect could be assigned to the higher binder dissolution from the bi-lumen tube already during extrusion due to the higher temperature of the extruded tube as it passes through the water in the cooling tank (8 °C) after the extrusion process. This higher temperature gradient already removes more binder of the tube and reduce the % Removal in the consecutive WD stage. The discussion has to be supported in the future with more replications.

The TD removes the remaining backbone binder components with a 1.56 % Removal, but did not show any significant variation in % Removal with extrusion parameters. The TD/PS produced surfaces without any damages that usually occur by binder expulsion in the form of vapour from the tubes. This fact shows that the selected TD/PS parameters were suitable for the micro parts. Still the PS samples were found to be very fragile and this fact suggests the use of a slightly higher PS temperature and holding time than the selected 800 °C and 1 hr for specimen handling purpose.

3.2 Surface quality

3.2.1 S_a variation at Green, WD and PS states

The surface roughness analysis of bi-lumen tubes showed quite wide variability both along the length and circumference directions of the tubes. So, an average of S_a values along the length and circumferential directions is considered as the representative value for each condition. The roughness analysis showed a general increase in the S_a value with respect to WD and PS as seen in Fig. 4. The increase in the S_a value from Green to WD state was very low, passing from an average S_a of 2.23 μm to 2.33 μm . The PS showed a higher S_a value of 2.62 μm , with an increase of 0.29 μm from the WD samples. The roughness variability completely covers these differences. The box plots showed that the variability of S_a values are higher at PS state than WD and Green, since the upper and lower whiskers being close to upper and lower quartiles respectively in PS state. This behavior is related to the binder component's behavior. WD removes the water soluble part but the backbone part of the binder remains even after WD. This fact keeps the surface roughness of the tube surface even after WD. In TD/PS state, the backbone part of the binder is removed completely leaving the pores fully open. This increases the roughness significantly in TD/PS state than in WD state.

3.2.2 S_a variation at Green, WD and PS states with respect to T_e and N_s levels

The variation of surface roughness with respect to the conditions used for extruding the bi-lumen tubes are studied with the Analysis of variance (ANOVA). The S_a main effects plot and interaction plot at Green (see Fig. 5a) showed that extrusion temperature and the $T_e N_s$ interaction are the important parameters for the extruded bi-lumen tubes roughness. ANOVA of S_a at Green showed the interaction $T_e N_s$ only as the significant extrusion variable with p-value < 0.05 (ANOVA assumptions are verified). The WD and PS samples seems to follow the same trend as the Green one even when the components of the binder are removed in each of these stages (see Fig. 5 b and c). The main effects plot and interaction plots of the WD state showed that extrusion variables extrusion temperature and $T_e N_s$ interaction have an influence on S_a .

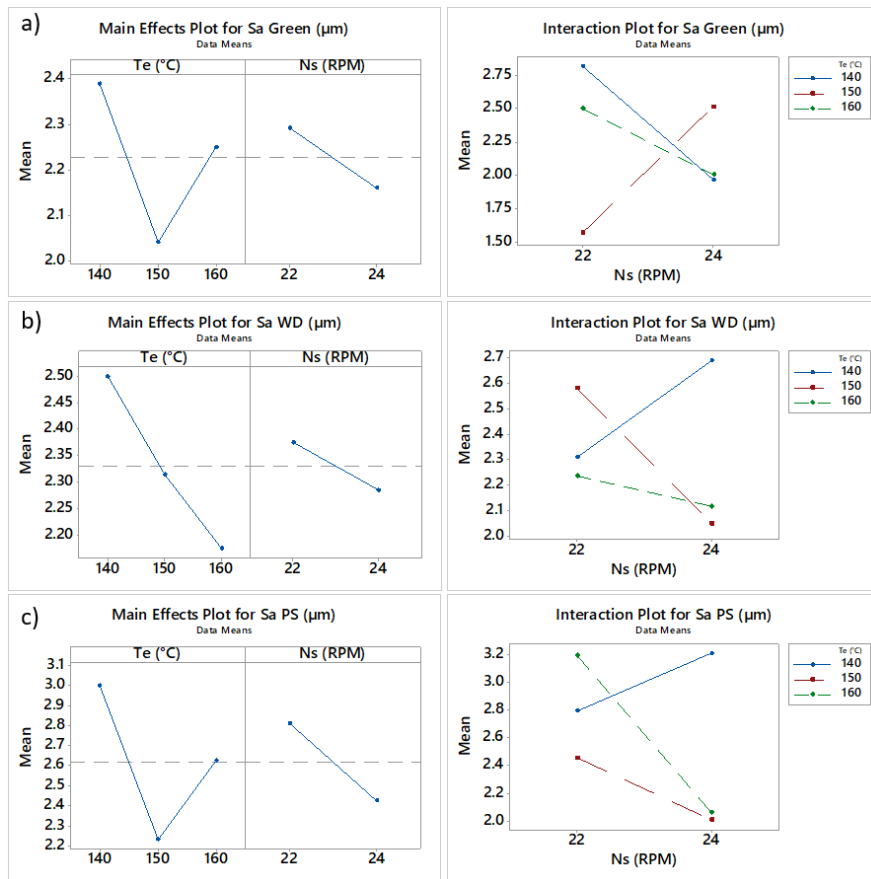


Fig. 5. Main effect and interaction plots of Sa with respect to the extrusion parameters Te and Ns at a) Green b) WD and c) PS states.

The ANOVA at WD state showed interaction Te*Ns only as the significant extrusion variable with p-value < 0.05 (assumptions are verified). The trend is more visible as the process chain moves to the PS state, where the binder is removed completely and the metal particle starts to attach by generating bonds. In addition to main effect plots and interaction plots, the ANOVA showed that extrusion temperature and interaction of Te*Ns are important for Sa at PS state (p-value < 0.05, assumptions verified). The analysis showed that Te*Ns as the most influencing factor. Extrusion temperature and extrusion velocity plays a role in the melting of the polymeric binder by direct heat transfer and also by shear melting. A right combination of Te*Ns is necessary as it regulate the viscosity and flow properties of the feedstock and also the surface finish.

3.3 The structural properties at Green, WD and PS states

The SEM analysis of the extruded bi-lumen tubes at Green shows generally sharp boundary reproduction for both tube and lumens. The cross-sectional analysis showed the retaining of good particle adhesion from the homogeneously distributed binder (that still should have all of its components) among the metal particles even after extrusion. WD removed the water-soluble component of the feedstock binder as a first phase in the binder removal process. The SEM images (Fig. 6 left) showed this difference with partial small agglomerated attachments because of the difference in the adhesion property at the cross section where the sample was broken for the analysis.

The SEM analysis of the tube cross-section and tube surfaces showed good quality without any damage. The tubes were devoid of any cracks or defects that usually occur during WD due to the dissolution of polymer from the feedstock. The surfaces after WD also did not show any corrosion of the metal particles as EDS didn't show oxides. This fact indicates that the selected solvent temperature of 50 $^{\circ}\text{C}$ and debinding time of 72 hrs were good enough to maintain the good surface finish without defects or corrosion for the extruded high-aspect-ratio micro bi-lumen tubes.

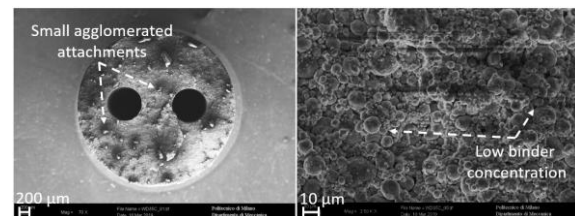


Fig. 6. SEM image of the bi-lumen tube cross-section at WD state

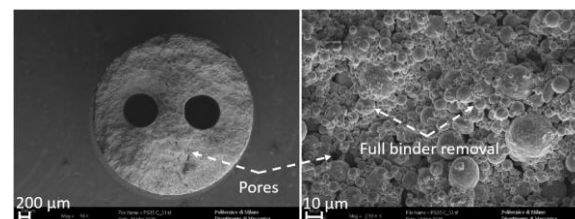


Fig. 7. SEM image of the bi-lumen tube cross-section at PS state

The SEM images of PS samples (see Fig. 7)

showed that TD and the following PS removed the last polymeric content of the feedstock. It evaporates before 600 °C and a TD holding time of 2.5 hrs assures the complete binder removal from the bi-lumen tubes leaving metal particles attached very loosely. Further heating at 4 °C/min and PS at 800 °C generate bonds between the bi-lumen tubes metal particles. The SEM images of the PS tubes showed the surfaces without any cracks or damages in the cross-section or at the surface, which is necessary in case of the debinding and PS of micro parts. The cross-section shows some opened pores. This fact is due to the free space created by the binder removal. The magnified SEM images of WD and PS samples (Fig. 8) clearly show the back bone binder attachments of the metal particles at the WD state and the bonding formation at the PS state.

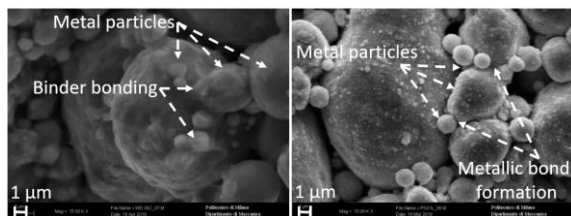


Fig. 8. SEM images of the metallic particle bonding at WD (left) and PS (right) states

3.3.2 Properties at the sintered state

One sample at the extrusion conditions extrusion temperature of 160 °C and extrusion velocity of 24 rpm was sintered as a representative sample (Mean Sa value was close to the grand mean values of the all the extrusion conditions at PS state) to qualitatively understand the final sintered properties of extruded bi-lumen tubes at the used WD and PS conditions. The SEM image of the cross section of the bi-lumen tube showed the nice structural integrity (see Fig. 9). The pores observed in the PS state were removed to a great extent by sintering. This fact proves the selected sintering parameters were suitable for the extruded bi-lumen tubes. Some pores were observed with the size of 1-6 µm in addition to some dark small globules with mainly Silicon and Oxygen content. This could possibly be due to some foreign particles observed in feedstock pellets and from the alloying elements in the steel.

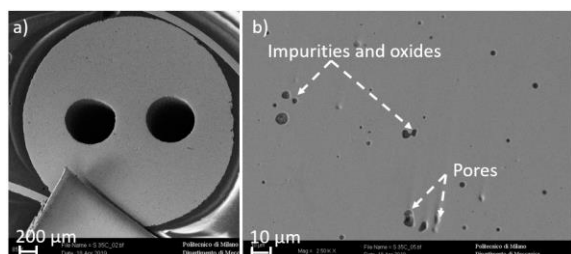


Fig. 9. SEM image of the bi-lumen tube cross-section at sintered state

The surfaces of sintered tubes showed a shining surface with good surface quality. The surface roughness of the sintered sample showed a Sa of 2.21 µm, which was close to the Sa at Green. The surfaces of the tubes did not show any cracks or defects. Sintering eliminated the porosity produced by debinding to a great extent but defects like extrusion marks were still retained on the surface even though in a diminished manner.

4. Conclusions

The debinding and pre-sintering study of the extruded micro bi-lumen tubes showed that the extrusion parameters influence their surface finish and properties. The extrusion parameters, extrusion temperature and interaction $T_e \cdot N_s$ influence the tubes surface roughness at green, WD and PS states. The experimented WD parameter levels; solvent temperature of 50 °C and debinding time of 48 hrs were found to be suitable for debinding with a good surface finish. A higher debinding time do not generate significant additional binder removal. The TD at 600 °C for 2.5 hrs and PS at 800 °C for 1 hr of the extruded bi-lumen tubes produced good surfaces without any cracks and proved suitable for processing of micro parts produced by feedstock extrusion. Sintering produced a good structural integrity with minimal pores and shows promising surface quality for bi-lumen tubes for the micro applications.

Acknowledgements

This research work was undertaken in the context of MICROMAN project ("Process Fingerprint for Zerodeflect Net-shape MICROMANufacturing", <http://www.microman.mek.dtu.dk/>). MICROMAN is a European Training Network supported by Horizon 2020, the EU Framework Programme for Research and Innovation (Project ID: 674801). Thanks go also to Dr. De Gaudenzi and Eng. Garabelli (Films S.p.a.), Eng. Fiorese and Mr. Gionda (TAV S.p.a.), Mr. Sanna and Eng. Alberti (Enki s.r.l.) and Eng. Mussi (MUSP) for their support.

References

- [1] U.M. Attia, et al., "A review of micro-powder injection moulding as a microfabrication technique," *J. Micromechanics Microengineering.*, 2011; 21: 1–22.
- [2] S.B. Li, et al., "Fabrication of thin-walled 316L stainless steel seamless pipes by extrusion technology", *J. Mater. Process. Technol.*, 2007; 183: 57–61.
- [3] G. Joamin, et al., "Additive manufacturing of metallic and ceramic components by the material extrusion of highly-filled polymers: A Review and Future Perspectives," *Materials.*, 2018; 11:840.
- [4] M.T. Zaky, "Effect of solvent debinding variables on the shape maintenance of green molded bodies," *J. Mater. Sci.*, 2004; 39: 3397–3402.
- [5] Y. Wu, et al., "Effects of residual carbon content on sintering shrinkage, microstructure and mechanical properties of injection molded 17-4 PH stainless steel," *J. Mater. Sci.*, 2002; 37: 3573– 3583.
- [6] M.F.F.A. Hamidi et al., "A review of biocompatible metal injection moulding process parameters for biomedical applications," *Mater. Sci. Eng. C.*, 2017; 78: 1263–1276.
- [7] X. Q. Liu, et al., "Deformation behavior and strength evolution of MIM compacts during thermal debinding," *Trans. Nonferrous Met. Soc. China (English Ed.)*, 2008; 18: 278–284.
- [8] J. Shi, et al., "Sintering of 17-4PH stainless steel powder assisted by microwave and the gradient of mechanical properties in the sintered body," *Int. J Adv. Manuf. Technol.*, 2017; 91:2895–2906.